

Quantum Averaging for High-Fidelity Quantum Logic Gates

Kristian D. Barajas^{1,2,3} and Wesley C. Campbell^{2,3}

¹*Mani L. Bhaumik Institute for Theoretical Physics*

University of California – Los Angeles, Los Angeles, California 90095, USA

²*UCLA Center for Quantum Science and Engineering (CQSE)*

University of California – Los Angeles, Los Angeles, California 90095, USA

³*Challenge Institute for Quantum Computation*

University of California – Berkeley, Berkeley, California 94720, USA

(Dated: March 1, 2025)

We present a two-timescale quantum averaging theory (QAT) for analytically modeling unitary dynamics in driven quantum systems. Combining the unitarity-preserving Magnus expansion with the method of averaging on multiple scales, QAT addresses the simultaneous presence of distinct timescales by generating a rotating frame with a dynamical phase operator that toggles with the high-frequency dynamics and yields an effective Hamiltonian for the slow degree of freedom. By retaining the fast-varying effects, we demonstrate the high precision achievable by applying this analytic technique to model a high-fidelity two-qubit quantum gate beyond the validity of first-order approximations. The results rapidly converge with numerical calculations of a fast-entangling Mølmer-Sørensen trapped-ion-qubit gate in the strong-field regime, illustrating QAT’s ability to simultaneously provide both an intuitive, effective-Hamiltonian model and high accuracy.

Quantum logic gates, the fundamental operations of quantum computation, perform operations on qubits akin to Boolean logic gates on classical bits [1]. However, physical realizations involve driving quantum systems over extended times where accurately modeling the unitary dynamics presents significant analytic and numerical challenge due to the presence of multiple timescales. For example, hardware-level interactions used to effect a basic X or Y gate can frequently be mapped onto a two-level system resonantly interacting with an AC electromagnetic field [2]. Under the rotating-wave approximation (RWA) [3] the AC field effectively induces coherent population inversion, which is essential for executing basic quantum logic gates. Without the RWA this seemingly simple example lacks an exact solution due to the presence of distinct timescales: the near-resonant Rabi oscillations overlaid with fast-varying beat note dynamics, leading to small gate imperfections.

Achieving fault tolerance will likely require a level of precision where fast-varying effects cannot be overlooked [1]. In classical dynamics, the fast and slow details are resolved with the two-timing method by introducing a slow “time” degree of freedom to regularize the approximate dynamics for long-time validity [4]. Two-timing has been shown [5] to provide equivalent results to a generalized method of averaging [6, 7] in which a near-identity transformation is generated into an effective equation of motion averaged over the fast degree of freedom. A two-timing (non-unitary) quantum framework was first proposed by Frasca [8] that produced robust analytic approximations for simple systems, but lacked the generality and an effective Hamiltonian description useful for practical applications. Although several advanced techniques exist to generate an “effective Hamiltonian” by averaging [9–13] or tracing over [14–17] high-frequency

effects, a generalized and unitary two-timescale approach for capturing the fast and slow details in driven quantum systems remains undeveloped.

In this Letter we introduce a two-timescale and unitary quantum averaging theory (QAT) and demonstrate its effectiveness in providing accurate gate fidelity estimates by applying it to the fast-entangling Mølmer-Sørensen gate [18] and demonstrating convergence with numerical calculations. The approach combines the unitarity-preserving Magnus expansion (ME) with the method of averaging (MA) on multiple scales valid for finite- and infinite-dimensional Hilbert spaces [19–21]. Full averaging with ME (and related high-frequency expansions) has been successful in high-frequency, periodic [22–25] and almost-periodic systems [26, 27]. In contrast, this approach performs “partial” averaging by effectively applying a low-pass filter over the fast degree of freedom to generate a rotating frame toggling with fast-varying effects such that the resulting effective Hamiltonian only depends on the slow degree of freedom. For detailed derivations and generalization to multiple timescales we refer to the companion paper [28].

I. THE TWO-TIMESCALE QUANTUM PERTURBATION PROBLEM

We consider weakly-perturbed quantum systems evolving under the Schrödinger-picture propagator $\hat{U}_S(s)$ satisfying Schrödinger’s equation for the total Hamiltonian $\hat{H}_S(s; \lambda) = \hat{H}_0(s) + \hat{V}(s; \lambda)$. Let $\hat{H}_0(s)$ be an exactly-solvable “unperturbed” Hamiltonian and $\hat{V}(s; \lambda) = \sum_{n=1}^{\infty} \lambda^n \hat{V}^{(n)}(s)$ be a bounded perturbation depending on a small parameter $0 \leq \lambda < 1$ [2, 20]. We define the dimensional time coordinate $s = \omega_0 t$, scaled by the characteristic frequency of the unperturbed system $\omega_0 \sim \|\hat{H}_0(t)\|/\hbar$. Following standard perturbative

treatment, the total propagator factorizes as $\hat{U}_S(s; \lambda) = \hat{U}_0(s) \hat{U}_I(s; \lambda)$ where the interaction propagator $\hat{U}_I(s; \lambda)$ is governed by the interaction Hamiltonian

$$\hat{H}_I(s; \lambda) = \sum_{n=1}^{\infty} \lambda^n \hat{H}_I^{(n)}(s), \quad \hat{H}_I^{(n)} = \hat{U}_0^\dagger \hat{V}^{(n)} \hat{U}_0 \quad (1)$$

and satisfies the interaction-picture Schrödinger equation

$$i \partial_s \hat{U}_I(s; \lambda) = \hat{H}_I(s; \lambda) \hat{U}_I(s; \lambda), \quad (2)$$

which remains to be solved. We assume the perturbation to be reasonably well-behaved as to be expanded in time-harmonic Fourier modes at one or more frequencies,

$$\hat{H}_I^{(n)}(s) = \hat{H}_{I,0}^{(n)} + \sum_{k=1}^{\mathcal{N}(n)} (e^{is\Lambda_{\omega_k}^{(n)}} \hat{h}_{I,k}^{(n)} + h.c.) \quad (3)$$

with $\mathcal{N}(n)$ total (dimensionless) base frequencies $\Lambda_{\omega_k}^{(n)} \doteq \omega_k^{(n)}/\omega_0$. Further, eq. (1) is presumed to characterize interactions occurring on at least two distinct timescales. The slow dynamics arise when a base frequency or a beat frequency, originating from higher-order interactions, approaches resonance. The resonant interactions dominate the long-time behavior, making them a natural candidate for inclusion in an effective Hamiltonian description.

The aim is to construct an effective Hamiltonian $\hat{\mathcal{H}}_{I,\text{eff}}(\tau; \lambda) = \sum_{n=1}^{\infty} \lambda^n \hat{\mathcal{H}}_{I,\text{eff}}^{(n)}(\tau)$ parameterized by a lagging “time” variable $\tau \doteq \lambda s$, characterizing the long-time $s \gtrsim \mathcal{O}(1/\lambda)$ interactions free from fast-varying effects. The effective Hamiltonian will govern an “effective” interaction picture equation for the slow-time (τ) dynamics from $\hat{H}_I(s; \lambda)$. The effective dynamics evolve under the effective propagator $\hat{U}_{\text{eff}}(\tau; \lambda)$ satisfying

$$i\lambda \partial_\tau \hat{U}_{\text{eff}}(\tau; \lambda) = \hat{\mathcal{H}}_{I,\text{eff}}(\tau; \lambda) \hat{U}_{\text{eff}}(\tau; \lambda) \quad (4)$$

where we’ve used $\partial_s = \lambda \partial_\tau$. Further, we wish to capture the influence rapidly-varying $s \lesssim \mathcal{O}(1)$ interactions have on the long-time dynamics. To generate the effective interaction picture we define an infinitesimal Lie transformation $\hat{U}_{\text{fast}}(s; \lambda)$ [6, 20, 29], known as the *fast propagator*, to transform (2) into (4). The interaction propagator is assumed to be in the QAT-factorized form

$$\hat{U}_I(s; \lambda) = \hat{U}_{\text{fast}}(s; \lambda) \hat{U}_{\text{eff}}(\tau; \lambda) \Big|_{\tau=\lambda s} \quad (5)$$

where the fast propagator characterizes the fast-varying modulations on the slowly-varying envelope of $\hat{U}_{\text{eff}}(\tau; \lambda)$.

II. THE QAT FORMALISM

To perturbatively generate the effective Hamiltonian we proceed with an asymptotic expansion. The standard approach is to generate the Lie transformation using a time-ordered Dyson series [2, 9–11, 29],

$$\hat{U}_{\text{fast}}(s; \lambda) = \hat{T} \left[e^{-i \int ds \hat{V}(s; \lambda)} \right] = \mathbb{1} + \sum_{n \geq 1} \lambda^n \hat{U}_{\text{fast}}^{(n)}(s), \quad (6)$$

which is no longer unitary upon truncation and produces non-Hermitian artifacts within the resulting effective Hamiltonian. Moreover, an approximate inverse propagator requires additional computational steps [6, 9]. Alternatively, an increasingly popular approach [23, 26, 27] is to use an exponential Lie transformation

$$\hat{U}_{\text{fast}}(s; \lambda) = \exp \left(-i \hat{\Phi}(s; \lambda) \right) \quad (7)$$

depending on a *dynamical phase* operator (or Magnus exponent) $\hat{\Phi}(s; \lambda) = \sum_{n=1}^{\infty} \lambda^n \hat{\Phi}^{(n)}(s)$ [19]. An immediate advantage of the exponential approach over the Dyson series is preservation of unitarity (enforcing the preservation of Hermiticity) upon truncation and providing a simple inverse property $(e^{i\hat{\Phi}})^{-1} = e^{-i\hat{\Phi}}$ [30].

After inserting eqs. (5) and (7) into (2), a Magnus expansion returns a homological equation of the form

$$\partial_s \hat{\Phi}^{(n)}(s) = \hat{\mathcal{H}}_{\Phi}^{(n)}(s) - \hat{\mathcal{H}}_{I,\text{eff}}^{(n)}(\tau) \quad (8)$$

where the auxiliary Hamiltonian operator $\hat{\mathcal{H}}_{\Phi}^{(n)}(s)$ is defined by a recursion relation provided in appendix (A). When solved, the integration constant can be ignored to remove any s_0 dependence, which imposes a uniqueness rule on the iterative Picard sequence and ensures the expansion is manifestly gauge invariant [24].

We employ a partitioned expansion by timescale separation (PETS) approach [28] based on a generalized method of averaging [6, 9, 29] valid for infinite-dimensional Hilbert spaces [20] such as with Fock space operators frequently used as a quantum bus [18, 31–33]. With the PETS approach, we separate $\hat{\mathcal{H}}_{\Phi}^{(n)}(s)$ into a fast-varying $\hat{\mathcal{H}}_{\Phi, >}^{(n)}(s)$, slow-varying $\hat{\mathcal{H}}_{\Phi, <}^{(n)}(s = \tau/\lambda)$, and constant $\hat{\mathcal{H}}_{\Phi, 0}^{(n)}$ contribution for a high-frequency cutoff $\lambda_{\text{cutoff}} = \lambda$ [34]. For a gauge-invariant and asymptotically valid QAT expansion, we require eq. (8) be regularized by demanding that

$$\overline{\hat{\Phi}^{(n)}(s)} = 0 \Leftrightarrow \hat{\Phi}^{(n)}(s) = \int_{-\infty}^s ds' \hat{\mathcal{H}}_{\Phi, >}^{(n)}(s') \quad (9a)$$

$$\hat{\mathcal{H}}_{\text{eff}}^{(n)}(\tau) = \overline{\hat{\mathcal{H}}_{\Phi}^{(n)}(s)} = \hat{\mathcal{H}}_{\Phi, 0}^{(n)} + \hat{\mathcal{H}}_{\Phi, <}^{(n)}(s = \tau/\lambda) \quad (9b)$$

where we use the “partial” time averaging procedure

$$\overline{\hat{A}(s)} = \hat{A}_0 + \hat{A}_{<}(s) \cong \int_{-\infty}^{\infty} ds' \hat{A}(s') f(s - s') \quad (10)$$

which removes fast-varying effects by effectively applying the RWA, *i.e.* an idealized low-pass filter $f(s)$ with a cutoff frequency λ . The regularizing conditions ensure $\hat{\Phi}(s; \lambda)$ reproduces the fast-varying dynamics and $\hat{H}_{\text{eff}}(\tau; \lambda)$ describes the slowly-varying interaction from $\hat{H}_I(s; \lambda)$. While the PETS approach shares many qualities with the low-pass filter formalism in Ref. [10], the

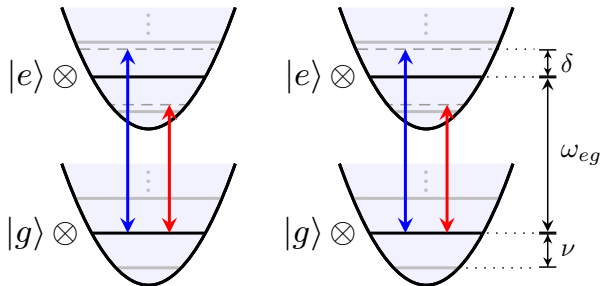


FIG. 1. Level diagram: Two ion qubits coupled to a single phonon mode, symmetrically driven near the first motional sidebands by red- ($-\delta$) and blue- ($+\delta$) detuned bichromatic drive.

QAT formalism doesn't suffer from non-unitary artifacts and retains the effects of high-frequency contributions. Further, the QAT expansion is guaranteed to be valid at each order in which the partitioning in eqs. (9a) and (9b) uniformly exist and is well-defined, which is assured for almost-periodic Fourier modes [5, 20]. Finally, $\hat{U}_I(s; \lambda)$ is approximated by the truncated QAT solution

$$\hat{U}_I^{[N]}(s; \lambda) = \hat{U}_{\text{fast}}^{[N-1]}(s; \lambda) \hat{U}_{\text{eff}}^{[N]}(\tau; \lambda) \Big|_{\tau=\lambda s} \quad (11)$$

for the time-evolution of the interaction picture state $|\psi_I^{[N]}(s; \lambda)\rangle = \hat{U}_I^{[N]}(s; \lambda) \hat{U}_I^{\dagger[N]}(s_0; \lambda) |\psi(s_0)\rangle$ where N is the truncation order, $\hat{U}_{\text{fast}}^{[N-1]}(s; \lambda) = \exp(-i\hat{\Phi}^{[N-1]}(s; \lambda))$, and $\hat{U}_{\text{eff}}^{[N]}(\tau; \lambda)$ is the exact or perturbative (up to $\mathcal{O}(\lambda^N)$) solution to $\hat{H}_{\text{eff}}^{[N]}(\tau; \lambda)$. Error bounds are discussed in [28].

III. EXAMPLE: FAST-ENTANGLING MØLMEER-SØRENSEN QUANTUM GATE

To demonstrate QAT, we consider a trapped-ion architecture consisting of ion qubits with atomic resonance frequency ω_{eg} allowed to oscillate along a single direction. The unperturbed system, $\hat{H}_0 = \hat{H}_{0, \omega_{eg}} + \hat{H}_{0, \nu}$, is composed of qubits, $\hat{H}_{0, \omega_{eg}} = \omega_{eg} \hat{J}_z$ where $\hat{J}_i = \sum_{n=1}^{N_{\text{ions}}} \sigma_i^{(n)}/2$ for $i = x, y, z$, and a phonon mode, $\hat{H}_{0, \nu} = \nu(a^\dagger a + 1/2)$, with secular frequency ν . In the fast-entangling operation proposed by Mølmer and Sørensen [18], a global bichromatic laser field $\hat{V}(t) = \frac{\Omega}{2} \sum_{l=R,B} \left(\hat{J}_+ e^{i\eta(\hat{a}^\dagger + \hat{a})} e^{-i(\omega_l t - \phi_l)} + h.c. \right)$ is applied where $\hat{J}_\pm = \hat{J}_x \pm i\hat{J}_y$, η is the Lamb-Dicke parameter, and $\omega_{B/R} = \omega_{eg} \pm \delta$ are equally Blue- ($+\delta$) and Red-detuned ($-\delta$) from resonance as seen in Fig. (1) [35].

Assuming $\omega_{eg} \gg \nu \gg \Omega$, we define $s = \nu t$, $\lambda = \Omega/\nu$, and $\Lambda_\omega \doteq \omega/\nu$ for any ω ($\Lambda_\nu = 1$) such that in the interaction picture of \hat{H}_0 [36],

$$\hat{H}_I(s) = \lambda f_c(s) \left((\hat{J}_{\phi,x} + i\hat{J}_{\phi,y}) \hat{\mathcal{D}}(\alpha(s)) + h.c. \right) \quad (12)$$

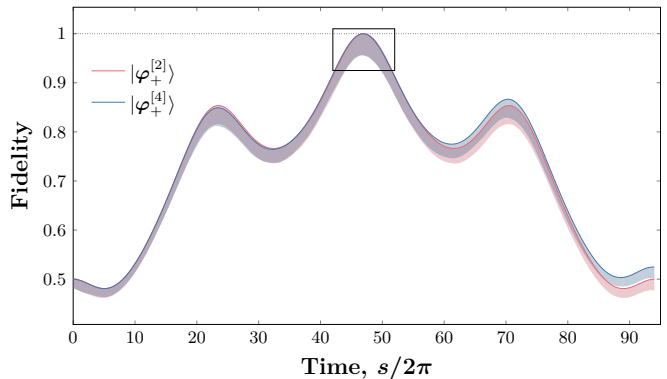


FIG. 2. **Low-frequency oscillations** for population in the Bell state $|\varphi_+\rangle = (|ee\rangle + |gg\rangle)/\sqrt{2}$ for two ion qubits interacting in a Mølmer-Sørensen gate. Prepared in the internal state $|gg\rangle$ and motional state $|0\rangle$, the ions are maximally entangled about time $s = \nu t = \pi\sqrt{2}\nu/\eta\Omega = 2\pi \times 47$. The physical parameters are $\eta = 0.1$, $\phi_+ = \pi/4$, and $\phi_- = 0$ with $\Omega \approx 0.15045\nu$ and $\delta \approx 0.9574\nu$ chosen to decouple from the first-order, off-resonant carrier transition at gate time. Both second-order (red) and fourth-order (blue) effective dynamics are in good agreement with the envelope of the numerical solution. The shading is a measure of the amplitude of the high frequency oscillations as seen in Fig. (3).

where $\hat{\mathcal{D}}(\alpha) = e^{\alpha\hat{a}^\dagger - \alpha^*\hat{a}}$ is the displacement operator, $\phi_\pm = (\phi_B \pm \phi_R)/2$, $f_c(s) = \cos(\Lambda_\delta s - \phi_-)$, $\alpha(s) = i\eta e^{is\Lambda_\nu}$, and $(\hat{J}_{\phi,x}, \hat{J}_{\phi,y}) = (\cos(\phi_+) \hat{J}_x - \sin(\phi_+) \hat{J}_y, \sin(\phi_+) \hat{J}_x + \cos(\phi_+) \hat{J}_y)$. Assuming $\eta/\lambda \sim \mathcal{O}(1)$, expanding $\hat{H}_I(s)$ in powers of λ yields

$$\hat{H}_I^{(n)}(s) = \begin{cases} 2if_c(s) \hat{J}_{\phi,y} \hat{\mathcal{D}}^{(n-1)}(\alpha(s)/\lambda), & n \text{ even} \\ 2f_c(s) \hat{J}_{\phi,x} \hat{\mathcal{D}}^{(n-1)}(\alpha(s)/\lambda), & n \text{ odd} \end{cases} \quad (13)$$

where $\hat{\mathcal{D}}^{(n)}(\alpha) = (\alpha\hat{a}^\dagger - \alpha^*\hat{a})^n/n!$ is the n th-order Taylor polynomial of the displacement operator (see appendix (B) for normal-ordered form). In the Lamb-Dicke regime we recover the familiar carrier ($n = 1$) and first motional sidebands ($n = 2$).

In contrast to an earlier slow-entangling protocol also by Mølmer and Sørensen [33], $\omega_{B/R}$ is tuned near the first motional sidebands, i.e. tuning Λ_δ near Λ_ν , such that the near-resonant interaction is parameterized by the low-frequency difference $\lambda\Lambda_\epsilon = \Lambda_\nu - \Lambda_\delta \leq \lambda$. From eq. (9), the second-order truncated QAT results yield

$$\hat{\Phi}^{[1]}(\sigma, \lambda) = 2\lambda \hat{J}_{\phi,x} \sin(\Lambda_\delta s - \phi_-)/\Lambda_\delta \quad (14a)$$

$$\hat{H}_{I,\text{eff}}^{[2]}(\tau; \lambda) = -\eta\lambda \hat{J}_{\phi,y} \hat{a}^\dagger e^{i(\Lambda_\epsilon \tau + \phi_-)} + h.c. \quad (14b)$$

where the latter admits the well-known solution [18]

$$\hat{U}_{\text{eff}}^{[2]}(\tau; \lambda) = \hat{\mathcal{D}} \left(\hat{J}_{\phi,y} \alpha_{\text{ms}}(\tau) \right) e^{i\vartheta(\tau) \hat{J}_{\phi,y}^2} \quad (15)$$

with $\alpha_{\text{ms}}(\tau) = \frac{2i\eta}{\Lambda_\epsilon} e^{i\phi_-} e^{i\Lambda_\epsilon \tau/2} \sin(\Lambda_\epsilon \tau/2)$ in the spin-dependent displacement operator and adiabatic phase

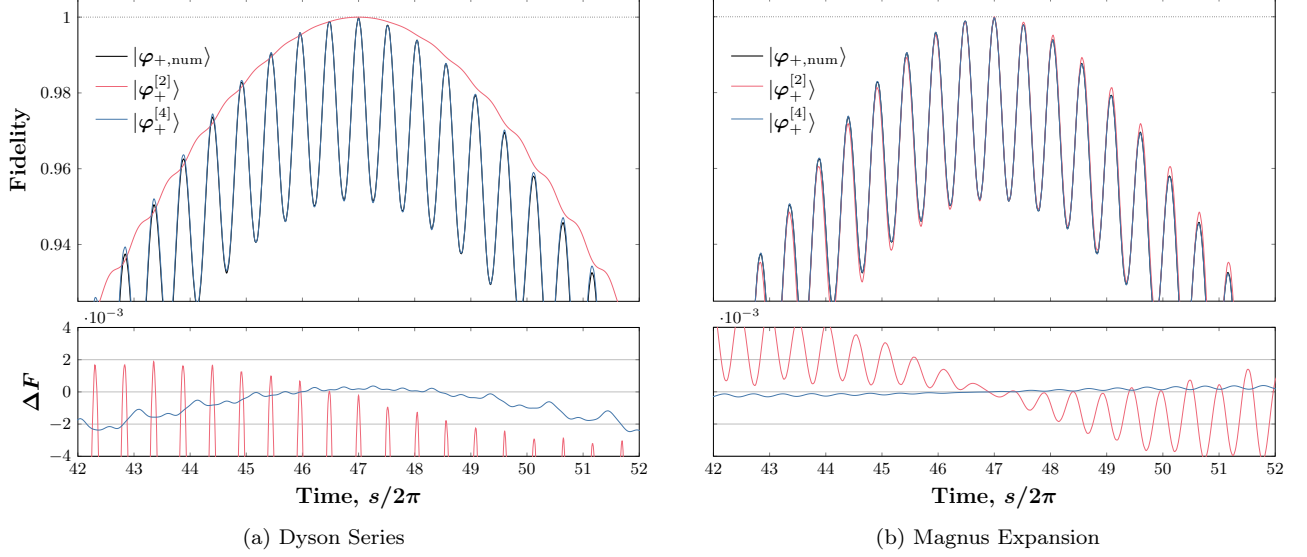


FIG. 3. **High frequency oscillations** located inside rectangular inset in Fig. (2) approximated by non-unitary (Dyson, left) and unitary (ME, right) QAT as compared with numerical integration (black). The deviation from numerical integration, $\Delta F = |\langle \varphi_+ | \psi_{I,\text{num}}(s) \rangle|^2 - |\langle \varphi_+ | \psi_I^{[N]}(s) \rangle|^2$, is shown in the lower plot. (a) Dynamics from Dyson kick propagator in appendix (D), approximately normalized due to being non-unitary and non-invertible. While the fourth-order result shows high frequency oscillations, the effects at second-order are nominal. (b) Dynamics from ME kick propagator discussed in this Letter. The high frequency oscillations are already well-characterized to second-order in unitary QAT.

$\vartheta(\tau) = \frac{\eta^2}{\Lambda_\epsilon^2} (\Lambda_\epsilon \tau - \sin(\Lambda_\epsilon \tau))$. The approximate QAT propagator, $\hat{U}_I^{[2]}(s; \lambda) = \exp(-i\hat{\Phi}^{[1]}(s; \lambda)) \hat{U}_{\text{eff}}^{[2]}(\tau; \lambda)|_{\tau=\lambda s}$, embodies all dynamics from $\hat{H}_I(s; \lambda)$ up to second order with bounded error estimate $\|\hat{U}_I(s; \lambda) - \hat{U}_I^{[2]}(s; \lambda)\| = \mathcal{O}(\lambda)$ over a time $s \sim \mathcal{O}(1/\lambda^2)$ [28].

The maximally-entangled Bell state $|\varphi_+\rangle = (|ee\rangle + |gg\rangle)/\sqrt{2}$ (up to a global phase) is ideally generated at time s_f if $\hat{U}_I(s_f, \lambda) = \exp(i\frac{\pi}{2}\hat{J}_{\phi,y}^2)$ for $\phi_+ = \pi/4$ and $\phi_- = 0$. From (15), this is effectively achieved for $\vartheta(\tau_f = \lambda s_f) = \pi/2$ and by waiting round trips in xp -phase space where $\alpha_{\text{ms}}(\tau_f) = 0$ and the coupling of the vibrational motion to the internal state is suppressed [18]. The well-known conditions are satisfied when $\Lambda_\epsilon \tau_f / 2\pi = (\Lambda_\nu - \Lambda_\delta) s_f / 2\pi = K \in \mathbb{N}$ and $\Lambda_\epsilon = 2\eta\sqrt{K}$. Higher fidelity is obtained by dynamically decoupling at gate time from off-resonant effects by demanding $\hat{\Phi}(s_f, \lambda) = 0$. To leading order, this occurs when $\Lambda_\delta s_f / \pi = K' \in \mathbb{N}$. In the “strong-field” regime shown in Fig. (3b), the high-frequency modulations reproduced to second-order (red) agree well with the numerical simulation (black) with $\Delta F_{\text{rms}} \simeq \pm 0.002$ within the inset, well within the $\mathcal{O}(\lambda)$ error bound. Accounting for $\hat{U}_{\text{fast}}(s; \lambda)$ reveals up to 4% increase in average gate fidelity. The results of unitary QAT are compared with the slower convergence of the Dyson fast propagator (see appendix (D)) in Fig. (3a).

We estimate subleading sources of fidelity loss to gate performance from corrections beyond the Lamb-Dicke regime. The dominant contributions to the effective Hamiltonian are from single-photon processes that ex-

cite the first motional sidebands through the net absorption/emission ($\hat{a}^\dagger \hat{a}^{\dagger n} \hat{a}^n / \hat{a}^{\dagger n} \hat{a}^n \hat{a}$) of a phonon given by the time-averaged interaction Hamiltonian $\hat{H}_I(\tau; \lambda) = i\lambda e^{-\eta^2/2} \hat{J}_{\phi,y} (\hat{C}_1(\eta) e^{i(\Lambda_\epsilon \tau + \phi_-)} - h.c.)$ where $\hat{C}_1(\eta) = \sum_{n \geq 0} \frac{(i\eta)^{2n+1}}{(n+1)!n!} \hat{a}^\dagger \hat{a}^{\dagger n} \hat{a}^n$. Smaller long-time effects include light shifts and multi-photon excitation of motional sidebands among increasingly complicated and weak interactions. For example, the next non-vanishing contribution to the effective Hamiltonian yields

$$\lambda^4 \hat{\mathcal{H}}_{\text{eff}}^{(4)}(\tau) = \frac{1}{2} \hat{J}_{\phi,y} \left\{ \hat{a}^\dagger e^{i(\Lambda_\epsilon \tau + \phi_-)} \left(\eta^3 \lambda (\hat{n} + 1) + \eta \lambda^3 / 2\Lambda_\delta'^2 \right) + h.c. \right\} - \frac{\eta^2 \lambda^2}{\Lambda_{\delta+\nu}} \hat{J}_{\phi,y}^2 \quad (16)$$

where $\Lambda_\delta'^2 = \frac{6\Lambda_\delta^2 \Lambda_{2\delta-\nu} \Lambda_{\delta+\nu}}{6\Lambda_\delta^2 + \Lambda_{\delta+\nu} \Lambda_{2\delta+\nu}} = \Lambda_\delta^2 + \mathcal{O}(\lambda)$. Note that the first motional sidebands are driven by a one-photon + three-phonon ($\eta^3 \lambda$) and a weakly-induced three-photon + one-phonon ($\eta \lambda^3$) excitation. The last term ($\eta^2 \lambda^2$) is an off-resonantly generated entangling interaction. The fourth-order contribution introduces a heightened sensitivity to heating, which affects the gates performance in the strong-driving regime.

We find that the asymptotic validity of the fast-entangling MS gate at second- and fourth-order depends on $\eta \lambda \sqrt{\hat{n} + 1} < \mathcal{O}(\lambda)$ and $\eta^3 \lambda (n + 1)^{3/2} / 2 < \mathcal{O}(\lambda^3)$, respectively, which for the parameters in Fig. (2) holds up to $\max(n) \lesssim 10$. With eqs. (14b) and (17), the fourth-order (τ -time) Magnus expansion [30] with the Zassen-

haus formula [37] yields

$$\hat{U}_{\text{eff}}^{[4]}(\tau; \lambda) = \hat{D}_2(-\eta^2/2\hat{J}_{\phi,y}\alpha_{\text{ms}}(\tau))e^{-2i\eta^2\vartheta(\tau)\hat{J}_{\phi,y}\hat{n}} \hat{D}(\hat{J}_{\phi,y}\alpha'_{\text{ms}}(\tau))e^{i\vartheta'(\tau)\hat{J}_{\phi,y}e^{\mathcal{O}(\lambda^5)}} \quad (17)$$

where $\alpha'_{\text{ms}}(\tau) = \alpha_{\text{ms}}(\tau)(1 - \frac{1}{2}[\lambda^2/\Lambda_\delta^2 + \eta^2])$, $\vartheta'(\tau) = \vartheta(\tau)(1 - [\lambda^2/\Lambda_\delta^2 + \eta^2]) + \eta^2\lambda\tau/\Lambda_{\delta+\nu}$, and $\hat{D}_2(\alpha) = e^{\alpha\hat{a}^\dagger\hat{n} - \alpha^*\hat{n}\hat{a}}$ is a quasi-displacement operator. While the vibrational motion largely decouples with the second-order condition $\tau_f = 2\pi K/\Lambda_\epsilon$, nonlinear spin-phonon coupling (i.e., $\hat{J}_{\phi,y}^2\hat{n}$) leaves a residual dependence on the vibrational quantum number n . Hence, optimum gate performance requires the modified temperature-dependent gate condition $\vartheta'(\tau_f) - 2\eta^2\vartheta(\tau_f)n + \mathcal{O}(\lambda^5) = \pi/2$. Alternatively, the gate performance can be made robust against heating for $\vartheta(\tau_f) = 0$ (i.e., $\vartheta'(\tau_f) = \frac{\eta^2\lambda}{\Lambda_{\delta+\nu}}\tau_f$) at the expense of the longer gate time $\tau_f = \pi\Lambda_\delta/\eta^2\lambda$, coinciding with the result of an earlier “weak-field” slow-entangling gate proposal [33]. To reproduce the fast, off-resonant dynamics to fourth order we include the dynamical phase contributions listed in Appendix (C). Unlike the second-order result, suppression of the higher-order, off-resonant interactions requires additional degrees of freedom such as pulse shaping of the bichromatic beam [38]. Without suppression, the result is an average fidelity loss of $\eta\lambda\sqrt{n+1}/2\Lambda_\delta$ (≈ 0.008). We find the fourth-order QAT propagator, $\hat{U}_I^{[4]}(s; \lambda) = \exp(-i\hat{\Phi}^{[3]}(s; \lambda))\hat{U}_{\text{eff}}^{[4]}(\tau; \lambda)|_{\tau=\lambda s}$, with bounded error estimate $\mathcal{O}(\lambda^3)$ over the gate time is in strong agreement with the results from numerical integration in Fig. (3b). For the given parameters, $\hat{U}_I^{[4]}(s; \lambda)$ estimates the gate fidelity to within $\Delta F_{\text{rms}} = \pm 0.0002$ inside the inset, comparable to the precision capabilities of state-of-the-art weak-field demonstrations [39–41].

In summary, we presented a unitarity-preserving, two-timescale QAT framework for analytically studying gate performance from slow- and fast-varying interactions. Notably, our approach distinguishes itself by retaining the details of the high-frequency dynamics, carried within a dynamical phase operator, while preserving unitarity and hermiticity. We demonstrated the robust characterization of gate dynamics and fidelity under strong spin-motion coupling for the fast-entangling Mølmer-Sørensen gate. For this example and others, the advantage of a scalable analytic and unitary framework is highlighted by the computational expense of numerical simulations of infinite-dimensional quantum systems such as harmonic oscillators, which are also prone to truncation errors. We expect the accurate modeling capabilities of QAT to enable enhanced control and manipulation for high-precision quantum computation.

The authors are deeply grateful to Robijn Bruinsma for helpful discussions and comments on the manuscript. We thank Alexander Radcliffe for the fruitful conversa-

tions on the Mølmer-Sørensen interaction in trapped-ion architectures.

Appendix A: QAT Recursion Relation

The auxiliary operator, $\hat{\mathcal{H}}_\Phi$, is defined as

$$\hat{\mathcal{H}}_\Phi = \hat{H}_I + \sum_{k \geq 1} \frac{B_k}{k!} \text{ad}_{i\hat{\Phi}}^{(k)} \left((-)^k \hat{H}_I - \hat{\mathcal{H}}_{I,\text{eff}} \right). \quad (18)$$

where B_k are Bernoulli numbers and the adjoint action $\text{ad}_{\hat{X}}(\hat{Y}) = [\hat{X}, \hat{Y}]$ and $\text{ad}_{\hat{X}}^{(k)}(\hat{Y}) = [\hat{X}, \text{ad}_{\hat{X}}^{(k-1)}(\hat{Y})]$ for integer $k \geq 2$. Expanding in λ , we find that the expansion coefficients $\hat{\mathcal{H}}_\Phi = \sum_{n \geq 1} \lambda^n \hat{\mathcal{H}}_\Phi^{(n)}$ are generated by

$$\hat{\mathcal{H}}_\Phi^{(n)} = \hat{H}_I^{(n)} + \sum_{k=1}^{n-1} \frac{B_k}{k!} \left((-)^k \hat{S}_k^{(n)} - \hat{T}_k^{(n)} \right) \quad (19)$$

where the operators $\hat{S}_k^{(n)}$ and $\hat{T}_k^{(n)}$ are generated by recurrence relations

$$\hat{S}_0^{(n)} = \hat{H}_I^{(n)}, \quad \hat{T}_0^{(n)} = \hat{\mathcal{H}}_{I,\text{eff}}^{(n)} \quad (20a)$$

$$\hat{A}_k^{(n)} = \sum_{m=1}^{n-k} \left[i\hat{\Phi}^{(m)}, \hat{A}_{k-1}^{(n-m)} \right], \quad 1 \leq k \leq n-1 \quad (20b)$$

where \hat{A} is to be replaced by \hat{S} or \hat{T} . The first three orders are provided for the reader’s convenience:

$$\begin{aligned} \hat{\mathcal{H}}_\Phi^{(1)} &= \hat{H}_I^{(1)} \\ \hat{\mathcal{H}}_\Phi^{(2)} &= \hat{H}_I^{(2)} + \frac{1}{2} [i\hat{\Phi}^{(1)}, \hat{H}_I^{(1)} + \hat{\mathcal{H}}_{I,\text{eff}}^{(1)}] \\ \hat{\mathcal{H}}_\Phi^{(3)} &= \hat{H}_I^{(3)} + \frac{1}{2} \left([i\hat{\Phi}^{(2)}, \hat{H}_I^{(1)} + \hat{\mathcal{H}}_{I,\text{eff}}^{(1)}] \right. \\ &\quad \left. + [i\hat{\Phi}^{(1)}, \hat{H}_I^{(2)} + \hat{\mathcal{H}}_{I,\text{eff}}^{(2)}] \right) \\ &\quad - \frac{1}{12} \left([i\hat{\Phi}^{(1)}, [i\hat{\Phi}^{(1)}, \hat{\mathcal{H}}_{I,\text{eff}}^{(1)} - \hat{H}_I^{(1)}]] \right) \end{aligned} \quad (21)$$

where explicit time dependence is omitted.

Appendix B: Formal Series Expansion of Displacement Operator

Expanding the time-periodic displacement operator in a Fourier series with $\theta = \Lambda_\nu s$ yields

$$\begin{aligned} \hat{\mathcal{D}}(\eta; \theta) &= e^{i\eta(\hat{a}^\dagger(\theta) + \hat{a}(\theta))}, \quad \hat{a}^\dagger(\theta) = \hat{a}^\dagger e^{i\theta} \\ &= \sum_{k \in \mathbb{Z}} \hat{\mathcal{D}}_k(\eta) e^{ik\theta} \end{aligned} \quad (22)$$

where

$$\begin{aligned} \hat{\mathcal{D}}_k(\eta) &= \frac{1}{2\pi} \int_{-\pi}^{\pi} e^{i\eta(\hat{a}^\dagger(\theta) + \hat{a}(\theta))} e^{-ik\theta} d\theta \\ &= e^{-\eta^2/2} \sum_{n=\frac{|k|-k}{2}}^{\infty} \frac{(i\eta)^{2n+k}}{(n+k)!n!} \hat{a}^{\dagger n+k} \hat{a}^n \\ &= e^{-\eta^2/2} \sum_{n=\frac{|k|-k}{2}}^{\infty} \hat{\mathcal{C}}_k^{(n)}(\eta) \end{aligned} \quad (23)$$

where $\hat{\mathcal{C}}_k^{(n)}(\eta) = \frac{(i\eta)^{2n+k}}{(n+k)!n!} \hat{a}^\dagger{}^{n+k} \hat{a}^n$ is a Bessel-Clifford polynomial operator satisfying $\hat{\mathcal{C}}_k^{(n)}(\eta) = \hat{\mathcal{C}}_k^{(n)}(-\eta) = (-1)^k \hat{\mathcal{C}}_k^{(n)}(\eta)$. Moreover, the formal exponential power series in powers of η returns

$$\begin{aligned} \hat{\mathcal{D}}(\eta; \theta) &= \sum_{n=0}^{\infty} \hat{\mathcal{D}}^{(n)}(\eta; \theta) \\ &= \sum_{n=0}^{\infty} \frac{(i\eta)^n}{n!} (\hat{a}^\dagger(\theta) + \hat{a}(\theta))^n. \end{aligned} \quad (24)$$

Using (23), the n th Taylor polynomial $\mathcal{D}^{(n)}(\theta)$ can be expressed in normal-ordered form as

$$\hat{\mathcal{D}}^{(n)}(\eta) = \sum_{m=0}^{\lfloor n/2 \rfloor} \sum_{k=-\ell}^{\ell} \frac{(i\eta)^n}{2^m m!} \hat{\mathcal{C}}_k^{(\frac{\ell-k}{2})}(1) e^{ik\theta} \quad (25)$$

where $\ell = n - 2m$ and $\lfloor x \rfloor$ is the greatest integer less than x .

Appendix C: Higher-Order Dynamical Phase Contributions to MS Gate Dynamics

The following are the dynamical phase contributions for the fast-entangling MS gate used in Fig. (3a):

$$\lambda^2 \hat{\Phi}^{(2)} = i \frac{\eta\lambda}{\Lambda_{\delta+\nu}} e^{i(\Lambda_{\delta+\nu}s - \phi_-)} \hat{J}_{\phi,y} \hat{a}^\dagger + h.c. \quad (26a)$$

$$\begin{aligned} \lambda^3 \hat{\Phi}^{(3)} &= \left\{ i\eta^2 \lambda \hat{J}_{\phi,x} (\hat{a}^\dagger)^2 e^{2i\Lambda_\nu s} \right. \\ &\quad \times \left(-\frac{e^{-i(\Lambda_\delta s - \phi_-)}}{2\Lambda_{\delta-2\nu}} + \frac{e^{i(\Lambda_\delta s - \phi_-)}}{2\Lambda_{\delta+2\nu}} \right) \\ &\quad - \frac{\eta\lambda^2}{2\Lambda_\delta^2} \hat{J}_z \hat{a}^\dagger e^{i\Lambda_\nu s} \left(\frac{e^{-2i(\Lambda_\delta s - \phi_-)}}{\Lambda_{\delta-\nu}} \right. \\ &\quad \left. + \frac{\Lambda_\nu e^{2i(\Lambda_\delta s - \phi_-)}}{\Lambda_{\delta+\nu}\Lambda_{2\delta+\nu}} + \frac{1}{\Lambda_{\delta+\nu}} \right) + h.c. \left. \right\} \\ &\quad - \frac{2\eta^2\lambda}{\Lambda_\delta} \sin(\Lambda_\delta s - \phi_-) \hat{J}_{\phi,x} (\hat{n} + 1/2). \end{aligned} \quad (26b)$$

Appendix D: Non-Unitary QAT from Dyson Expansion of Fast Propagator

Using the standard Dyson series expansion in eq. (6), the algebraic-derived homological equation is [6]

$$\begin{aligned} i\partial_s \hat{U}_{\text{fast}}^{(n)}(s) &= \hat{H}_I^{(n)}(s) - \hat{\mathcal{H}}_{\text{eff}}^{(n)}(\tau) \\ &\quad + \sum_{k=1}^{n-1} \left(\hat{H}_I^{(k)}(s) \cdot \hat{U}_{\text{fast}}^{(n-k)}(s) \right. \\ &\quad \left. - \hat{U}_{\text{fast}}^{(k)}(s) \cdot \hat{\mathcal{H}}_{\text{eff}}^{(n-k)}(\tau) \right), \end{aligned} \quad (27)$$

which only preserves unitarity (and Hermiticity of $\hat{\mathcal{H}}_{\text{eff}}(\tau, \lambda)$) in the infinite resummation of all orders. While arguably simpler to implement, the computational

overhead can be quite large at higher orders compared to the recursive algorithm in (19). Moreover, since the truncated Dyson fast propagator is non-unitary and difficult to invert, the quantum state must be approximately normalized, for example, to initial conditions with $|\psi_I^{[N]}(s, \lambda)\rangle \simeq |\psi_{I, \text{Dyson}}^{[N]}(s, \lambda)\rangle / \|\psi_{I, \text{Dyson}}^{[N]}(s_0, \lambda)\|$ where $|\psi_{I, \text{Dyson}}^{[N]}(s, \lambda)\rangle = \hat{U}_{\text{fast}}^{[N-1]}(s, \tau, \lambda) \hat{U}_{\text{eff}}^{[N]}(\tau, \lambda)|_{\substack{s=s \\ \tau=\lambda s}} |\psi_0\rangle$.

In the case of the fast-entangling Mølmer-Sørensen gate presented in this Letter, the effective Hamiltonian from non-unitary QAT is given by

$$\hat{\mathcal{H}}_{\text{eff}}^{(1)} = \hat{\mathcal{H}}_{\text{eff}}^{(3)} = 0 \quad (28a)$$

$$\lambda^2 \hat{\mathcal{H}}_{\text{eff}}^{(2)}(\tau) = -\eta\lambda \hat{J}_{\phi,y} \hat{a}^\dagger e^{i(\Lambda_\epsilon \tau + \phi_-)} + h.c. \quad (28b)$$

$$\begin{aligned} \lambda^4 \hat{\mathcal{H}}_{\text{eff}}^{(4)}(\tau) &= \frac{1}{2} \hat{J}_{\phi,y} \left\{ \hat{a}^\dagger (\eta^3 \lambda (1 + \hat{n}) - \eta\lambda^3 / \Lambda_\delta^2) \right. \\ &\quad \times e^{i(\Lambda_\epsilon \tau + \phi_-)} + h.c. \left. \right\} - \frac{\eta^2 \lambda^2}{2\Lambda_\delta} \hat{J}_{\phi,y}^2 \\ &\quad + 2i \frac{\eta\lambda^3}{\Lambda_\delta^2} \hat{J}_{\phi,x} \hat{J}_z (\hat{a}^\dagger e^{i(\Lambda_\epsilon \tau + \phi_-)} + h.c.), \end{aligned} \quad (28c)$$

which is closely similar to the result from unitary QAT with small differences at fourth-order due to a non-Hermitian artifact. The expansion coefficients of the Dyson series fast propagator are given by

$$\lambda \hat{U}_{\text{fast}}^{(1)} = -2i\lambda \hat{J}_{\phi,x} \sin(\Lambda_\delta s - \phi_-) / \Lambda_\delta \quad (29a)$$

$$\begin{aligned} \lambda^2 \hat{U}_{\text{fast}}^{(2)} &= -\frac{\eta\lambda}{2\Lambda_\delta} \hat{J}_{\phi,y} \left(\hat{a}^\dagger e^{i(2\Lambda_\delta s + \Lambda_\epsilon \tau - \phi_-)} - h.c. \right) \\ &\quad + \frac{\lambda^2}{2\Lambda_\delta^2} \hat{J}_{\phi,x}^2 \cos(2\Lambda_\delta s - 2\phi_-) \end{aligned} \quad (29b)$$

$$\begin{aligned} \lambda^3 \hat{U}_{\text{fast}}^{(3)} &= \frac{\eta^2 \lambda}{2\Lambda_\delta} \hat{J}_{\phi,x} \left(\{ (\hat{a}^\dagger)^2 e^{i(\Lambda_\delta s + 2\Lambda_\epsilon \tau)} (e^{i\phi_-} \right. \\ &\quad \left. + e^{i(2\Lambda_\delta s - \phi_-)} / 3) - h.c. \} \right. \\ &\quad \left. + 4i \sin(\Lambda_\delta s - \phi_-) (\hat{n} + 1/2) \right) + \\ &\quad i \frac{\eta\lambda^2 \Lambda_\epsilon}{4\Lambda_\delta^2} \hat{J}_{\phi,y} \left(\hat{a}^\dagger e^{i(2\Lambda_\delta s + \Lambda_\epsilon \tau - \phi_-)} - h.c. \right) \\ &\quad + \frac{\eta\lambda^2}{2\Lambda_\delta^2} \hat{J}_{\phi,x} \hat{J}_{\phi,y} \left(\hat{a}^\dagger e^{i(\Lambda_\delta s + \Lambda_\epsilon \tau)} \right. \\ &\quad \left. \times \{ 1 - e^{2i(\Lambda_\delta s - \phi_-)} \} + h.c. \right) + \\ &\quad - i \frac{\lambda^3}{2\Lambda_\delta^3} \hat{J}_{\phi,x}^3 (\sin(\Lambda_\delta s - \phi_-) \\ &\quad + \sin(3\Lambda_\delta s - 3\phi_-) / 3) \\ &\quad + i \frac{\eta\lambda^2}{\Lambda_\delta^2} \hat{J}_z \left\{ \hat{a}^\dagger e^{i(\Lambda_\delta s + \Lambda_\epsilon \tau)} (e^{-2i(\Lambda_\delta s - \phi_-)} \right. \\ &\quad \left. + e^{2i(\Lambda_\delta s - \phi_-)} / 3) + h.c. \right\}. \end{aligned} \quad (29c)$$

The comparatively slower convergence of non-unitary QAT are shown in Fig. (3).

-
- [1] M. A. Nielsen and I. L. Chuang, *Quantum Computation and Quantum Information: 10th Anniversary Edition* (Cambridge University Press, 2010).
- [2] J. J. Sakurai and J. Napolitano, *Modern Quantum Mechanics* (Cambridge University Press, 2020).
- [3] C. J. Foot, *Atomic Physics*, Oxford Master Series in Physics (Oxford University Press, Oxford, New York, 2005).
- [4] S. H. Strogatz, *Nonlinear Dynamics and Chaos: With Applications to Physics, Biology, Chemistry, and Engineering*, 2nd ed. (CRC Press, Boca Raton, 2019).
- [5] L. M. Perko, *SIAM Journal on Applied Mathematics* **17**, 698 (1969), 2099314.
- [6] A. A. Kamel, *Celestial Mechanics* **3**, 90 (1970).
- [7] J. Sanders, F. Verhulst, and J. Murdock, *Averaging Methods in Nonlinear Dynamical Systems*, Applied Mathematical Sciences, Vol. 59 (Springer, New York, NY, 2007).
- [8] M. Frasca, *Il Nuovo Cimento B (1971-1996)* **107**, 915 (1992).
- [9] W. Scherer, *Physics Letters A* **233**, 1 (1997).
- [10] D. F. James and J. Jerke, *Canadian Journal of Physics* **85**, 625 (2007).
- [11] H. Jauslin, S. Guérin, and S. Thomas, *Physica A: Statistical Mechanics and its Applications* **279**, 432 (2000).
- [12] D. Zeuch, F. Hassler, J. J. Slim, and D. P. DiVincenzo, *Annals of Physics* **423**, 168327 (2020), arXiv:1807.02858 [quant-ph].
- [13] M. Bukov, L. D'Alessio, and A. Polkovnikov, *Advances in Physics* **64**, 139 (2015), arXiv:1407.4803 [cond-mat].
- [14] J. R. Schrieffer and P. A. Wolff, *Physical Review* **149**, 491 (1966).
- [15] M. Sanz, E. Solano, and Í. L. Egusquiza, in *Applications + Practical Conceptualization + Mathematics = Fruitful Innovation*, edited by R. S. Anderssen, P. Broadbridge, Y. Fukumoto, K. Kajiwara, T. Takagi, E. Verbitskiy, and M. Wakayama (Springer Japan, Tokyo, 2016) pp. 127–142.
- [16] V. Paulisch, H. Rui, H. K. Ng, and B.-G. Englert, *The European Physical Journal Plus* **129**, 12 (2014).
- [17] M. Te Vrugt and R. Wittkowski, *Physical Review E* **99**, 062118 (2019).
- [18] A. Sørensen and K. Mølmer, *Physical Review A* **62**, 022311 (2000).
- [19] W. Magnus, *Communications on Pure and Applied Mathematics* **7**, 649 (1954).
- [20] R. Buitelaar, *The Method of Averaging in Banach Spaces: Theory and Applications*, Ph.D. thesis, Universiteit Utrecht, Netherlands (1993).
- [21] A. H. Nayfeh, in *Perturbation Methods* (John Wiley & Sons, Ltd, 2000) Chap. 6, pp. 228–307.
- [22] S. Rahav, I. Gilary, and S. Fishman, *Physical Review A* **68**, 013820 (2003).
- [23] F. Casas, J. A. Oteo, and J. Ros, *Journal of Physics A: Mathematical and General* **34**, 3379 (2001).
- [24] A. Eckardt and E. Anisimovas, *New Journal of Physics* **17**, 093039 (2015).
- [25] N. Goldman and J. Dalibard, *Physical Review X* **4**, 031027 (2014).
- [26] F. Casas, *European Journal of Physics* **36**, 055049 (2015).
- [27] A. Arnal, F. Casas, and C. Chiralt, *Mathematical and Computational Applications* **25**, 50 (2020).
- [28] K. D. Barajas and W. C. Campbell, Unpublished. (2024).
- [29] J. R. Cary, *Physics Reports* **79**, 129 (1981).
- [30] S. Blanes, F. Casas, J. A. Oteo, and J. Ros, *Physics Reports* **470**, 151 (2009), arXiv:0810.5488 [math-ph].
- [31] K. D. Petersson, L. W. McFaul, M. D. Schroer, M. Jung, J. M. Taylor, A. A. Houck, and J. R. Petta, *Nature* **490**, 380 (2012).
- [32] J. Majer, J. M. Chow, J. M. Gambetta, J. Koch, B. R. Johnson, J. A. Schreier, L. Frunzio, D. I. Schuster, A. A. Houck, A. Wallraff, A. Blais, M. H. Devoret, S. M. Girvin, and R. J. Schoelkopf, *Nature* **449**, 443 (2007).
- [33] A. Sørensen and K. Mølmer, *Physical Review Letters* **82**, 1971 (1999).
- [34] More generally, the frequency cutoff must obey $\lambda \leq \lambda_{\text{cutoff}} < 1$ with improved results for $\lambda \leq \lambda_{\text{cutoff}} \ll 1$ [28].
- [35] For simplicity, we have disregarded the optical counter-rotating terms $\propto 2\omega_{eg}$ appearing in the interaction picture. Leading order corrections are of strength $\mathcal{O}(\Omega/2\omega_{eg}) \ll 1$, which for $\omega_{eg} \gg \nu \gg \Omega$ are significantly smaller than the perturbative regime probed.
- [36] The system is sequentially transformed, first with respect to $\hat{H}_{0,\omega_{eg}}$ and then $\hat{H}_{0,\nu}$, then scaled by the secular frequency.
- [37] F. Casas, A. Murua, and M. Nadinic, *Computer Physics Communications* **183**, 2386 (2012), arXiv:1204.0389 [math-ph, physics:quant-ph].
- [38] M. Sameti, J. Lishman, and F. Mintert, *Physical Review A* **103**, 052603 (2021).
- [39] C. J. Ballance, T. P. Harty, N. M. Linke, M. A. Sepiol, and D. M. Lucas, *Physical Review Letters* **117**, 060504 (2016).
- [40] J. P. Gaebler, T. R. Tan, Y. Lin, Y. Wan, R. Bowler, A. C. Keith, S. Glancy, K. Coakley, E. Knill, D. Leibfried, and D. J. Wineland, *Physical Review Letters* **117**, 060505 (2016).
- [41] C. R. Clark, H. N. Tinkey, B. C. Sawyer, A. M. Meier, K. A. Burkhardt, C. M. Seck, C. M. Shappert, N. D. Guise, C. E. Volin, S. D. Fallek, H. T. Hayden, W. G. Rellergert, and K. R. Brown, *Physical Review Letters* **127**, 130505 (2021).